Significance and evaluation of Poisson's ratio in Rayleigh wave testing

Mourad Karray and Guy Lefebvre

Abstract: Important progress has been made in the past 20 years in the use of surface-wave testing in soil characterization. However, the effect of Poisson's ratio on the construction of the theoretical dispersion relationships, associated with the inversion process, has not received enough attention and remains poorly documented. Five ideal profiles with different degrees of variation of shear-wave velocity with depth and three published case records are considered in this paper to study the effect of Poisson's ratio on Rayleigh wave phase velocities. The effect of the variation of Poisson's ratio on the evaluation of shear-wave velocity profiles (V_s) is also examined. Poisson's ratio is generally assumed in surface-wave testing, and therefore the paper also examines the possibility of evaluating its value using a multi-mode inversion process. The results of surface-wave testing obtained at two experimental sites are then used to illustrate the potential of surface-wave testing to evaluate the Poisson's ratio profile in addition to the V_s profile. The impact of Poisson's ratio in Rayleigh wave testing is shown to be significantly more important than previously demonstrated. The error resulting from Poisson's ratio does not depend solely on the magnitude of the inaccuracy. A multi-mode inversion process is shown to be a useful tool to determine the Poisson's ratio profile, leading to a more accurate soil characterization.

Key words: Poisson's ratio, surface waves, Rayleigh waves, shear-wave velocity, compression-wave velocity, modal analyses.

Résumé : Au cours des 20 dernières années, on a réalisé des progrès important dans l'utilisation des essais basés sur les ondes de surface pour la caractérisation des sols. Toutefois, l'effet du coefficient de Poisson sur la construction des relations théoriques de dispersion, associées au processus d'inversion, n'a pas reçu suffisamment d'attention et demeure mal documenté. Dans cet article, cinq profils idéals avec différents degrés de variation de la vitesse des ondes de cisaillement et trois cas expérimentaux publiées ont été considérés pour étudier l'effet du coefficient de Poisson sur la vitesse de phase des ondes de Rayleigh. L'article examine également l'effet de la variation du coefficient de Poisson sur l'évaluation des profils de vitesse des ondes de cisaillement (V_s). En général, la valeur du coefficient de Poisson est assumée dans les essais basées sur les ondes de surface, et en conséquence, l'article examine aussi la possibilité d'évaluer sa valeur au moyen d'un processus d'inversion multi-mode. Les résultats des essais d'onde de surface obtenus à deux sites expérimentaux sont utilisés pour illustrer le potentiel de l'essai d'onde de surface pour évaluer le profil du coefficient de Poisson en plus du profil de V_s. On montre que l'impact du coefficient de Poisson dans les essais basés sur les ondes de Rayleigh est plus important que ce qui a été démontré antérieurement. L'erreur résultant du choix du coefficient de Poisson ne dépend pas seulement de la grandeur de l'inexactitude. On montre qu'un processus d'inversion multi-mode est un outil efficace pour déterminer le profil du coefficient de Poisson menant à une caractérisation plus précise du sol.

Mots-clés : coefficient de Poisson, ondes de surface, ondes de Rayleigh, vitesse des ondes de cisaillement, vitesse des ondes de compression, analyses modales.

[Traduit par la Rédaction]

Introduction

The elastic properties of soils measured at low strain ($<10^{-3}$), such as shear modulus (G_{max}), Young's modulus (E_{max}), or Poisson's ratio (ν), are essential parameters for dynamic response analysis and soil–structure interaction problems and can play an important role in the study of liquefaction potential under seismic loading (Youd et al. 2001). These parameters are also useful for the characterization of soils in terms of geotechnical and mechanical properties (Robertson et al. 1995). The shear-wave velocity (V_s) or shear modulus ($G_{max} = \rho V_s^2$, where ρ is the mass density) can be used for in situ evaluation of hard-to-sample deposits and eventually for identification of bedrock position. It can also be used to derive in situ density (Stokoe et al. 1994), stress conditions, or in situ strength and large-strain behavior of granular soils (Robertson et al. 1995). Poisson's ratio (ν) or compression-wave velocity (V_p) are good indicators of the depth of saturation in deposits.

However, the dynamic elastic parameters need to be accurately determined for use in geotechnical engineering. For example, when the density index (I_d) is evaluated from the relation proposed by Seed and Idriss (1970), namely:

$$[1] \qquad I_d = kV_s^2 - 25, \quad k = \frac{\rho_{tot}}{1.336 \times 10^5 (\sigma'_m)^{1/2}}$$

where σ'_m is the mean effective stress and ρ_{tot} is the density

Received 29 September 2006. Accepted 11 January 2008. Published on the NRC Research Press Web site at cgj.nrc.ca on 13 May 2008.

M. Karray[1] and G. Lefebvre. Department of Civil Engineering, Faculty of Engineering, Université de Sherbrooke, Sherbrooke, QC J1K 2R1, Canada.

[1]Corresponding author (e-mail: mourad.karray@usherbrooke.ca).

of material (kg/m^3), an error of 10% in V_s produces an error greater than 25% in I_d.

Although crosshole and downhole seismic surveys have long been used for evaluation of dynamic properties of soil, spectral analysis of surface waves (SASW), developed in the early 1980s, has opened the way for V_s profiling without the need for any boring or sounding. The SASW method (Nazarian and Stokoe 1985) involves two steps: (*i*) determination of the dispersion curve (phase velocity versus wavelength) and (*ii*) transformation of this dispersion curve into a shear-wave velocity profile using an inversion process. In the first step, the phase velocity between two sensors located at given distances from an impact source is evaluated as a function of frequency or wavelength (λ). The test is repeated for several receiver spacings to cover a wide wavelength band and in two directions to account for the effects of deposit variability. Heisey (1982) proposed filtering criteria suggesting that the acceptable wavelengths must be between $d/2$ and $3d$ (where d is the receiver spacing). An overall dispersion curve is then obtained by the application of the same process for all receiver spacings considered. In the second step, the average dispersion curve is transformed into a shear-wave velocity profile (inversion) by comparing the experimental dispersion curve with the theoretical curve corresponding to the fundamental Rayleigh mode calculated for a horizontally stratified medium consisting of N layers.

Because the measurements are made at the surface without the need for boring or sounding, the SASW method has generated great interest. However, the method can, in some cases, be affected by reliability or accuracy problems. In SASW, the experimental dispersion curve is assumed to be representative of the fundamental Rayleigh mode only. However, a number of experimental and analytical studies have demonstrated that, in some conditions, higher modes can interfere and even dominate the fundamental Rayleigh mode and thus significantly affect the dispersion curve, even if the source and sensor locations in the standard SASW procedure are designed to minimize the contribution of the higher modes.

The problem of higher Rayleigh mode contribution to the dispersion curve in surface-wave testing was identified fairly early (Jones 1958) but was believed for many years to be associated only with deposits characterized by an irregular V_s profile, i.e., a profile where V_s does not increase regularly with an increase in depth (Tokimatsu et al. 1992; Gucunski and Woods 1992; Ganji et al. 1998). More recently, however, detailed numerical analysis of seismic-wave propagation in response to an impact at the ground surface has shown that higher Rayleigh modes can contribute to the dispersion curve even for deposits with a regular V_s profile and even when using SASW criteria (Karray 1999). Today, there is consensus that methods of investigation based on surface waves should assume that higher Rayleigh modes can contribute to the dispersion curve and that techniques should be used to separate or eliminate the contribution of these higher modes before proceeding with inversion (Lefebvre and Karray 1998; Park et al. 1999; Foti 2000).

The assumed Poisson's ratio can also be a source of inaccuracy because it must be assumed in each layer in the inversion process. It is well known that the effect of Poisson's ratio is not very important in an elastic, homogeneous, and isotropic medium. The ratio (k_r) between phase velocity (V_R) and V_s varies from 0.91 for $\nu = 0.20$ to 0.95 for $\nu = 0.50$ (Richart et al. 1970). A two-layer system, consisting of a layer of soft material underlain by a stiffer half-space (Fig. 1) with a shear-wave velocity contrast of 1.5, has been considered by Nazarian (1984) to study the effect of Poisson's ratio on construction of the theoretical dispersion curve. The results shown in Fig. 1 (using the same example considered by Nazarian) indicate that over a range of Poisson's ratios of 0.15–0.49, normalized velocities at a given wavelength vary no more than about 10%. On this basis, it can be concluded that the Poisson's ratio does not introduce a significant error in construction of the dispersion curve if it is reasonably assumed. Considering the field conditions that are generally encountered, the homogeneous half-space (Richart et al. 1970) and the example of Fig. 1 (Nazarian 1984) are, however, not sufficient for a general conclusion on the effect of ν on the theoretical calculation of the dispersion curve in the inversion process. The objectives of this paper are (*i*) to evaluate the effect of Poisson's ratio in the inversion process for conditions similar to those generally encountered in the field, when V_s varies with depth; and (*ii*) to describe how Poisson's ratio can be evaluated through Rayleigh wave testing using more than one mode in the inversion process.

Description of the procedures

Transforming a dispersion curve into a shear-wave velocity profile (inversion) using the Rayleigh wave testing method consists of comparing the experimental dispersion curve with one that is theoretically constructed for a horizontally stratified medium consisting of N layers. Each layer is assumed to be isotropic, homogeneous, and characterized by thickness (h), mass density (ρ), Poisson's ratio (ν), and shear-wave velocity (V_s). The process is repeated until the computed and experimental curves match.

Theoretical dispersion

The first step in the inversion process involves the construction of the theoretical dispersion curves (Rayleigh modes in the case of multi-modal inversion). The dispersion problem consists of determining function roots and can be formulated, for a given stratified medium, by the equation

$$[2] \qquad \Delta(\lambda, c, \{X\}) = 0, \qquad X = \{V_{s_1}, h_1, \rho_1, \nu_1, \ldots\ldots, V_{s_n}, h_n, \rho_n, \nu_n\}$$

where λ is the wavelength, c is the phase velocity, and Δ is the dispersion function and can be constructed using different techniques (Haskell 1953; Knopoff 1964; Dunkin 1965; Aki and Richardson 1980; Kausel and Roësset 1981). The optimization of Knopoff's method for computer application by Schwab (1970) is used in this study. For a given frequency or wavelength, the first root of the dispersion function corresponds to the fundamental Rayleigh mode, and the nth root to the $(n - 1)$th mode. In this study, the roots of the function Δ are determined using the secant method. In fact, the process began by bracketing the first root (fundamental mode) of the function Δ corresponding to the lower wavelength using a simple transformation, $c_1 = 0.93k_rV_{smin}$ and $c_2 = 0.96k_rV_{smin}$. The term V_{smin} corresponds to the lower

Fig. 1. Effect of Poisson's ratio on dispersion curve (recalculated from the same data used by Nazarian (1984)).

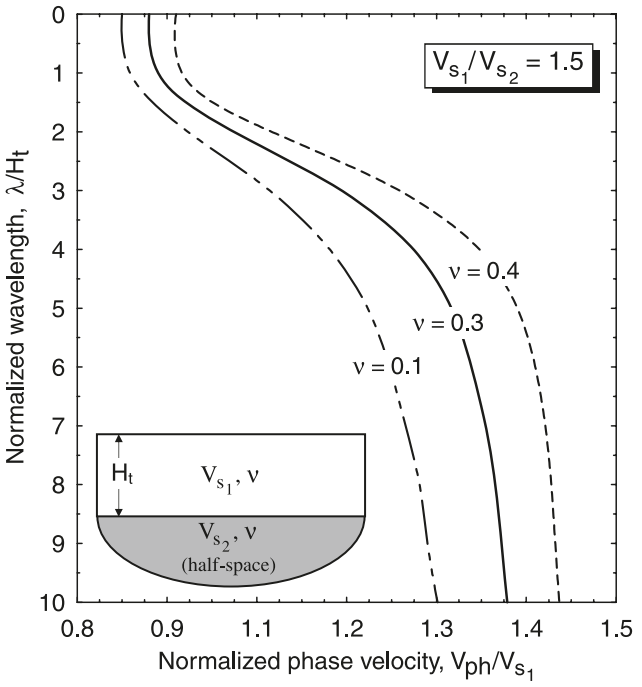

shear-wave velocity in the medium; and the ratio k_r, between c and V_s, varies from 0.91 for $\nu = 0.2$ to 0.95 for $\nu = 0.50$ (Richart et al. 1970). It should be noted that the process is applied for the geological model only and for c lower than the shear-wave velocity of the half-space. The nth root for the same Rayleigh mode is then bracketed using the $(n - 1)$th root. The process is repeated for the other roots of higher modes (Karray 1999).

Multi-mode inversion

To evaluate the shear-wave velocity profile and the corresponding compression-wave velocity or Poisson's ratio profile, the fundamental Rayleigh mode is first inverted by assuming a Poisson's ratio for each layer considered. The theoretical first Rayleigh mode or the available higher mode is then evaluated and compared to the experimental mode. The process is then repeated with a new compression-wave velocity profile until the theoretical and experimental modes match.

The automated inversion process developed by Karray (1999) has been used in this study. In this procedure, the minimization of the difference between the theoretical and experimental dispersion curves proceeds not only in terms of phase velocity but also in terms of the shape of the dispersion curves, allowing more rapid convergence and also better detection of the weaker or stronger layers at given depths (Karray 1999). The inversion is accomplished by linearization $[\Phi']^{\text{iteration}}$ of the system at each step of the process.

The difference (phase and shape) between the experimental and theoretical modes, $\Delta c'$, is minimized using the simplex method (Nelder and Mead 1964). Convergence is controlled by the least-squares criteria. The intermediate solution is also controlled at each step. Thus, when an intermediate solution leads to a difference, Δc (phase only) containing an opposite sign, this solution is penalized. The solution is accepted when the difference between the experimental and theoretical modes, Δc, is lower than 1% for all the wavelengths considered in the process.

Impact of Poisson's ratio on phase velocity

Analytical solutions

The dispersion relation for a Gibson half-space, which is defined as a compressible half-space of constant density and with a shear modulus increasing linearly with an increase in depth ($G = \rho V_s^2 = G_0(mz + 1)$, where G is the shear modulus, z is the depth, and $G_0 = \rho V_{s_0}$), has been derived for various values of Poisson's ratio by Vardoulakis and Vrettos (1988) and can be written using the formula:

$$[3] \qquad c(\lambda) \approx V_{s_0}\sqrt{\frac{0.568(\nu + 1.5)m\lambda + 2.857}{(3.6 - \nu)}}, \qquad \lambda \leq \frac{0.88(3.6 - \nu)}{(1.5 + \nu)}\left(\frac{c}{mV_{s_0}}\right)$$

where m is a measure of nonhomogeneity, $m = 0$ corresponds to a homogeneous half-space; and V_{s_0} is the shear-wave velocity at the surface of the medium. Equation [3] is applicable for ν varying between 0.25 and 0.50 and for small values of λ. Based on this equation, the difference ξ (in %) in phase velocity between $\nu = 0.49$ and 0.33, for a Gibson half-space, can be expressed as

$$[4] \qquad \xi \approx 100\left(1 - \sqrt{\frac{0.364m\lambda + 0.919}{0.318m\lambda + 0.874}}\right)$$

Equation [4] indicates that the error that can be introduced in construction of the dispersion curve depends on the wavelength and the degree of nonhomogeneity of the medium. For example, for a wavelength $\lambda = 1$ m, the error introduced between $\nu = 0.49$ and 0.33 is about 5.2% for $m = 4$ and 3.7% for $m = 1$. For a wavelength $\lambda = 4$ m, the error is about 6.4% and 5.2%, respectively. Although the model of eq. [3] cannot be applied for large λ, this example only serves to show that the error produced by the Poisson's ratio increases with an increase in wavelength and the degree of nonhomogeneity of the medium.

Parametric study — ideal cases

This parametric study documents the impact of Poisson's ratio on construction of the dispersion curve, and ultimately, on the inversion process.

To parametrically study the effect of Poisson's ratio on construction of the theoretical dispersion curve, five illustrative systems composed of eight layers underlain by a stiff half-space are considered. Case 1 represents a non-dispersive soil profile, while cases 2–5 represent soil profiles where the shear-wave velocity increases linearly with the increase in depth according to the following formula: $V_s = V_{s_0} + \Delta_v z$, where Δ_v is the rate of increase of V_s with depth, with Δ_v = 2, 4, 8, and 16 m·s^{-1}/m, respectively. The shear-wave velocity at the free surface of the medium (V_{s_0}) is 50 m/s in all cases. A constant density ρ

Table 1. Typical values of Poisson's ratio (ν), after Sharma et al. (1990) and Davidovici (1985).

Type of material	Sharma et al.	Davidovici
Saturated clay	0.40–0.5	0.5
Nonsaturated clay	0.10–0.3	
Medium clay	—	0.40–0.45
Sandy clay	0.20–0.30	0.35–0.4
Silt	0.30–0.35	—
Sand, gravelly sand	0.30–0.40	0.25–0.30
Silty sand, clayey sand	—	0.30–0.35
Rock	0.10–0.40	—
Concrete	0.15	—

of 1900 kg/m^3 is considered for all the layers and for the half-space.

Theoretical dispersion curves are evaluated for the different profiles, assuming values of Poisson's ratio of 0.20, 0.33, and 0.49. According to Sharma et al. (1990) and Davidovici (1985), these values represent the lower, average, and higher (saturated soil) values of ν that can be encountered in different soil material (Table 1). In each case, the Poisson's ratio is the same for all the layers and also for the half-space. The percentage of difference between phase velocities calculated for $\nu = 0.33$, which is taken as the reference value, and those evaluated for $\nu = 0.20$ and 0.49 are presented in Fig. 2 as a function of wavelength, normalized using the total height of the media (H_t).

For the homogeneous nondispersive media ($\Delta_v = 0$, case 1), the relative difference in phase velocities is about 2% and does not change with wavelength, as indicated in Richart et al. (1970). In cases of dispersive soils, phase velocity is affected by wavelength as well as by degree of V_s increase with the increase in depth (Δ_v).

The relative difference in phase velocity with respect to $\nu = 0.33$ varies significantly with wavelength, especially for $\Delta_v = 8$ and 16 m·s^{-1}/m. The difference converges, at a normalized wavelength lower than 0.2, to the difference obtained for the nondispersive media. Beyond $\lambda/H_t = 0.2$, the relative difference increases quasi-linearly with normalized wavelength and reaches a maximum (5%–15%) at a value of λ/H_t varying between 2 and 3. At a value of λ/H_t greater than 2 or 3, the relative difference remains constant or decreases slowly with an increase in wavelength, depending on the value of Δ_v. It is interesting to note that the relative difference between $\nu = 0.20$ and 0.33 varies in approximately the same manner with wavelength, as that between 0.33 and 0.49 for Δ_v, equal to 2 and 4 m·s^{-1}/m, respectively, and differs for $\Delta_v = 8$ and 16 m·s^{-1}/m. For $\Delta_v = 16$ m·s^{-1}/m, the maximum difference is reached at a normalized wavelength of about 2 for $\nu = 0.20$ and about 3 for $\nu = 0.49$.

The difference between the examples presented in this study and those dealt with by Nazarian (1984) is the degree of variation of shear-wave velocity with depth (Δ_v). Results for the two layers of Nazarian's example are reproduced in Fig. 2 for comparison purposes and are between $\Delta_v = 0$ and 2 m·s^{-1}/m. It should be noted that the increase in velocity with an increase in depth simply due to the mean effective overburden stress ($(\sigma'_{v0})^{1/4}$) can be greater than 8 m·s^{-1}/m in the first 10 m. For example, for a given density index, I_d, of 75% and ρ of 2000 kg/m^3, the increase in velocity between 9 and 10 m depth in the same soil deposit, according to eq. [1], is 8.14 m·s^{-1}/m in nonsaturated soil and 6.8 m·s^{-1}/m in saturated soil. The average value of Δ_v between the first and the tenth metre is 15.2 m·s^{-1}/m in the case of nonsaturated soil and 12.76 m·s^{-1}/m in the case of saturated soil.

To appreciate the importance of the parameter Δ_v, the relative difference in phase velocity with respect to $\nu = 0.33$ is presented in Fig. 3 as a function of Poisson's ratio for different values of Δ_v (i.e., 0, 2, 4, 8, and 16 m·s^{-1}/m) and for normalized wavelengths (λ/H_t) of 1 and 2. The typical values of ν given in Table 1 (Davidovici 1985; Sharma et al. 1990) for different soil materials are also illustrated in Fig. 3. The relative difference varies quasi-linearly with the Poisson's ratio, with a rate that increases proportionally with the degree of nonhomogeneity of the media (Δ_v). In fact, for large values of Δ_v and λ ($\Delta_v = 16$ m·s^{-1}/m and $\lambda/H_t = 2$), the difference seems to converge to a maximum of about 12% for $\nu = 0.50$ and about 23% for $\nu = 0.10$.

Case records

To illustrate the effect of Poisson's ratio on construction of the theoretical dispersion curve, three experimental shear-wave velocity profiles from the literature are considered (Fig. 4). The first profile (case 1) was obtained by Addo and Robertson (1994) at Richmond Dykes (Blundell Road) in Richmond, B.C. The second case (case 2) was published by Stokoe et al. (1994), and the third (case 3) was evaluated according to the relation proposed by Hardin and Drnevich (1972) to reflect only the effective overburden stress ($(\sigma')^{1/4}$). In the first case, the shear-wave velocity increases slowly with an increase in depth at a rate of approximately 3 m·s^{-1}/m in the first two layers and 6 m·s^{-1}/m in the deeper layers. In the second case, V_s increases by more than 25 m·s^{-1}/m in the first 4 m and by 16 m·s^{-1}/m between 4 and 20 m. In the third case, V_s increases at a rate of 16 m·s^{-1}/m between 0 and 4 m and decreases rapidly at a given depth (3 m·s^{-1}/m).

The theoretical dispersion curves are evaluated for Poisson's ratios of 0.20, 0.33, and 0.49, and the relative differences with the reference value of 0.33 are presented in Fig. 5.

As indicated by the parametric study (Fig. 2), the difference in phase velocity related to Poisson's ratio becomes more important as the degree of V_s increases with an in-

Fig. 2. Effect of Poisson's ratio on dispersion curve for different shear-wave velocity rates (m).

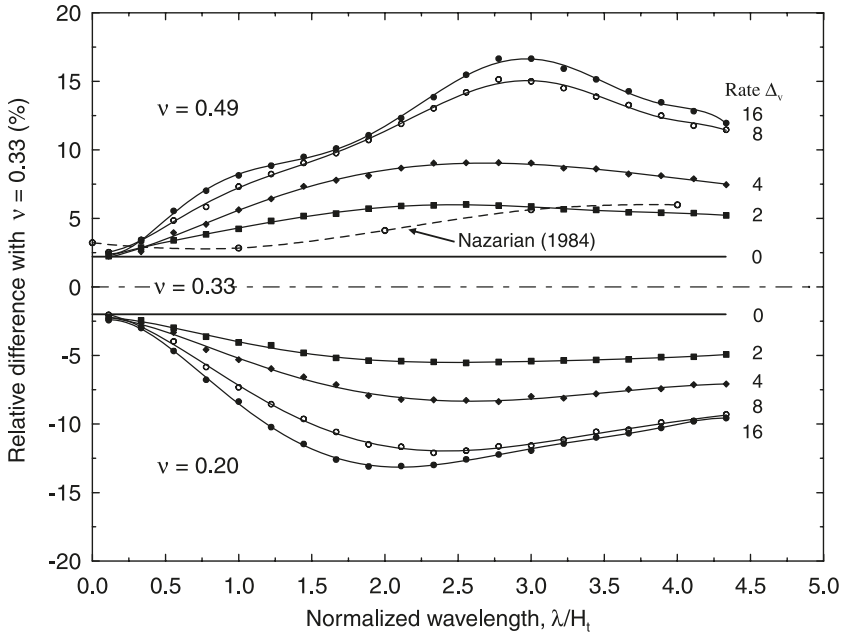

Fig. 3. Variation of relative difference of phase velocities with ν for λ/H_t = 1 and 2.

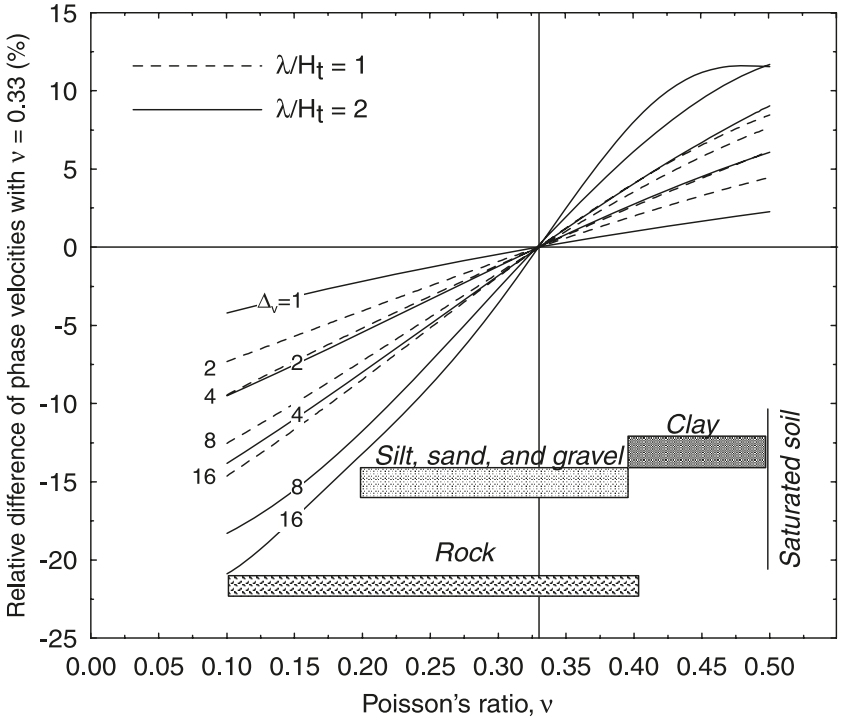

crease in depth (Δ_v). The difference in phase velocity, as compared with that for ν = 0.33, varies from 2.5% to 8.5% for case 1, from 5% to 18% for case 2, and from 2.5% to 10% for case 3 (Fig. 5). In fact, the variation in the degree of V_s increase with an increase in depth (Δ_v) in the same profile seems to play a leading role in the variation of phase velocity with variation of Poisson's ratio. When the rate of V_s increase is important in the upper layers, the effect of the Poisson's ratio becomes more important. The difference in case 3 (Δ_v = 3 m·s^{-1}/m at $2H_t/3$) is about 10% at a normalized wavelength of 3 (Fig. 5), as compared with 7% in the ideal case for Δ_v = 4 m·s^{-1}/m (Fig. 2). In case 2, the difference reaches a maximum of 18% (for ν = 0.49) at a normalized wavelength of 2 (Fig. 5) compared with 10% in the ideal case for Δ_v = 16 m·s^{-1}/m (Fig. 2). The reverse effect is also true, as demonstrated by case 1 with a difference of 8.5% at a normalized wavelength of 3 (Fig. 5) compared with approximately 10% in the ideal case with Δ_v =

Fig. 4. Typical shear-wave velocity profiles.

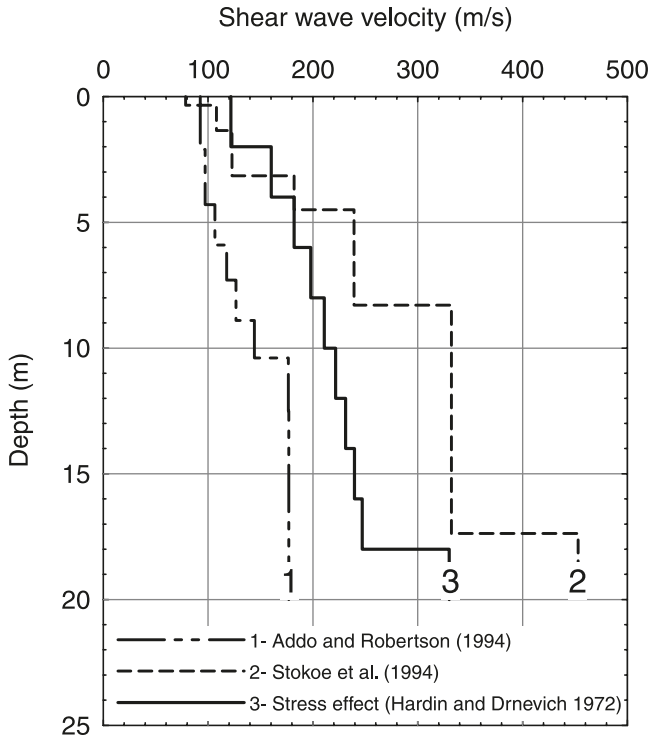

6 m·s^{-1}/m (Fig. 2). This is explained by the fact that near-surface layers have an important effect on the dispersion curve even at large wavelengths because of the nature of the Rayleigh waves, which decay exponentially with an increase in depth.

Impact of Poisson's ratio on shear-wave velocity

Figure 6*a* shows the shear-wave velocity profiles determined for the same experimental dispersion curve (R-0, Fig. 6*c*) but for three different values of ν of 0.20, 0.33, and 0.49. It should be noted that the thickness of the layer increases with an increase in depth (0.5 m for the first four layers, 1.33 m for the fifth layer, and 1.66 m for the last four layers overlaying the half-space). Relative differences between the profiles evaluated with ν = 0.20 and 0.49 and the profile evaluated with ν = 0.33 (Fig. 6*a*) are shown in Fig. 6*b*.

In both cases (ν = 0.20 and 0.49), the relative variation of V_s, as compared with that for ν = 0.33, is important at certain depths (variation >15%–20%). In fact, the relative difference varies in a fairly regular way for ν = 0.49 compared with that for ν = 0.20 (Fig. 6*b*). This implies that the problem of inversion varies in a nonlinear way with the variation of Poisson's ratio. Thus, even if there is a difference of about 5%–15% in terms of V_s, for a Poisson's ratio of 0.49, the form of the V_s profile is preserved in general. However, the use of a Poisson's ratio of 0.20 instead of 0.33 leads to a more important difference in V_s, which varies with depth by between 0% and 30%, and thus induces a distortion in the shape of the V_s profile. Distortion in the shape of the profile with variation of Poisson's ratio can lead to problems of interpretation. Figure 6*a* shows the existence of a stiffer layer between depths of 1.0 and 3.5 m if a value of 0.20 is retained for ν. However, this zone does not exist if a Poisson's ratio of 0.49 or 0.33 is used. This example shows that the solution of the inversion process using only the fundamental Rayleigh mode can lead to a different solution depending on the choice of ν profile.

Figure 6*c* shows the dispersion curves for the fundamental mode (R-0) used in the inversion process to obtain the profiles of Fig. 6*b*. Figure 6*c* also shows the dispersion curves for the first higher Rayleigh mode determined for each set of V_s profiles obtained with different values of ν (Fig. 6*a*). Figure 6*c* shows the difference between the fundamental and first higher mode change with the variation of Poisson's ratio profile. Thus, the determination from the field records of at least one higher Rayleigh mode, in addition to the fundamental mode, would make it possible to evaluate the Poisson's ratio profile and eventually determine an accurate and optimal solution.

Evaluation of Poisson's ratio

The correct isolation of the fundamental Rayleigh mode (R-0) is important to determine a reliable shear-wave velocity profile. However, this is not sufficient to arrive, in the inversion process, at a V_s profile, which could be considered an optimal solution because it varies with the choice of ν, as demonstrated in Figs. 6*a* and 6*b*. However, the determination of a higher Rayleigh mode (R-*n*), or at least part of it, in addition to R-0, could help evaluate the compression-wave velocity or the Poisson's ratio profile. A method for the isolation of the fundamental and higher Rayleigh modes contributing to the field records is described later in the text.

Multi-mode dispersion relations

The records are first analyzed using the multiple filter technique proposed by Dziewonski et al. (1969). The multiple filter technique is used to examine the energy distribution in a time–frequency domain and provides information about the different groups of waves participating in the tests. The technique consists of the filtration of the field records for a narrow frequency band centred around ω_n, where ω_n is the central frequency of the filter, and the computation of the local maximums of the envelope of the filtered signals. The multiple filter technique is a suitable method to evaluate the group velocity dispersion curve of the different Rayleigh modes in surface-wave records (Lefebvre and Karray 1998) and eventually to verify the dominance of the fundamental mode. The group velocity, V_g, corresponds to the propagation velocity of the maximum energy and is related to the phase velocity, V_{ph}, as follows:

$$[5] \qquad V_g = V_{ph} - \lambda \mathrm{d}V_{ph}/\mathrm{d}\lambda$$

If the fundamental mode is not dominant throughout the frequency range of interest, it must be isolated to obtain a representative phase velocity dispersion curve. The time-variable filter technique can be used to isolate the fundamental and also the existing higher Rayleigh modes (Lefebvre and Karray 1998). The purpose of the time-variable filter is to strongly reduce or eliminate the energy

Fig. 5. Relative difference of phase velocity for the different typical shear-wave velocity profiles of Fig. 4.

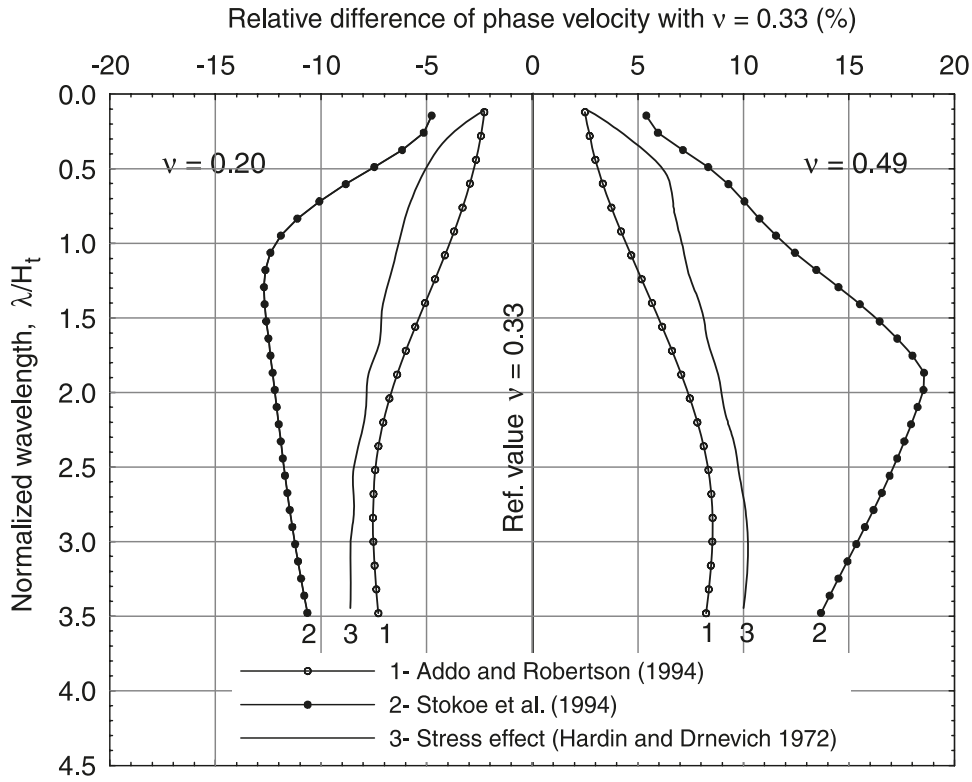

Fig. 6. (*a*) Shear-wave velocity profiles calculated for the same fundamental Rayleigh mode (Fig. 6*c*) and for different values of ν. (*b*) Relative difference between shear-wave velocities for different values of ν. (*c*) Fundamental and first Rayleigh modes corresponding to the set of V_s profiles (Fig. 6*a*) and the corresponding Poisson's ratio.

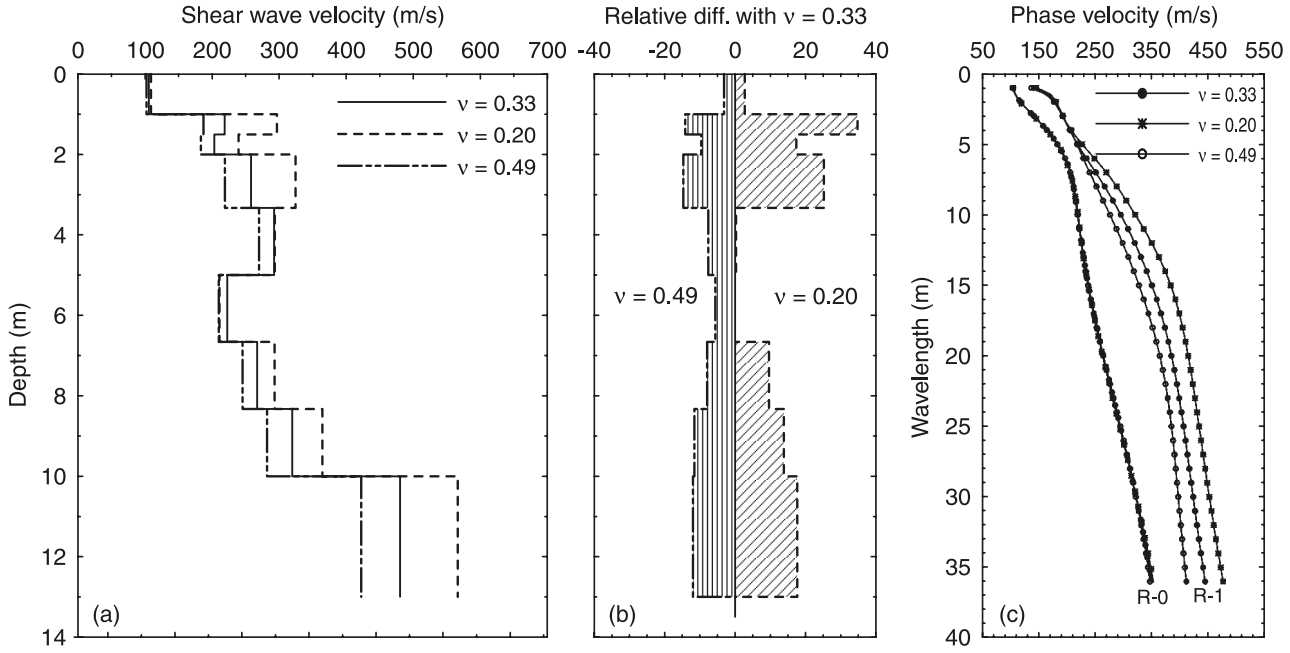

of any mode or wave type that does not belong to the selected wave group. If the group velocity or travel-time dispersion relationship of a given mode is known (multiple filter technique), it is possible to design a filter such that only the energy of the selected group is transmitted.

Experimental sites

SASW test records at two experimental sites are used to illustrate the separation of Rayleigh modes and their use in a multi-mode inversion process.

Saint Alban site

The SASW tests were performed in November 1990 on a soft Champlain Sea deposit in Saint Alban, Que., 80 km west of Québec City on the north shore of the St. Lawrence River (Lefebvre et al. 1994). The soil profile consists of 0.3 m of topsoil; 1.2–1.5 m of weathered clay crust; 8.0 m of soft silty clay, becoming more silty with depth; 4.0 m of clayey silt with sand; and a deep layer of dense sand (La Rochelle et al. 1974). The water table was reported at a depth of 0.75 m. The tests, conducted according to the SASW configuration (Nazarian 1984) with receiver spacings of 4, 8, and 16 m, were initially analyzed by Lefebvre et al. (1994), assuming that the fundamental Rayleigh mode was dominant. Reanalysis of the field records, using the multiple filter and the time-variable filter techniques, indicates that the participation of the first higher modes, in this case, is not very important. Figure 7 compares the fundamental and first higher modes determined by the filtration techniques with the dispersion points obtained according to the SASW criteria. The filtered dispersion curve representing the fundamental mode coincides approximately with that of unfiltered SASW for wavelengths greater than 5 m. For wavelengths less than 5 m, however, the SASW dispersion points are affected by the first higher Rayleigh mode.

In Lefebvre et al. (1994), a Poisson's ratio of 0.3 was erroneously considered for the entire deposit, assuming at the time that this parameter did not have a significant effect on construction of the theoretical dispersion curve. The dispersion curves of the fundamental and first higher Rayleigh modes, computed using the multiple filter and time-variable filter techniques, are compared in Fig. 8 with those evaluated theoretically for two shear-wave velocity profiles: (*i*) one obtained by the inversion of the fundamental Rayleigh mode using a Poisson's ratio of 0.20 for the first metre and 0.49 below that, and (*ii*) the second with $\nu = 0.30$ as used by Lefebvre et al. The experimental filtered first higher mode is in good agreement, in the available range of frequencies (17–35 Hz), with the theoretical mode obtained with the proposed Poisson's ratios ($\nu = 0.20$ and 0.49). The theoretical mode obtained with a constant Poisson's ratio of 0.30 also agrees with the experimental filtered mode between frequencies of 22 and 35 Hz, but differs slightly for frequencies between 17 and 22 Hz (λ between 3.5 and 5.0 m).

Even if the contribution of higher Rayleigh modes is not very important in this case, the scatter associated with the participation of the first mode at short wavelengths results in an average dispersion curve that has a different shape from that of the filtered dispersion curve (Fig. 7), which

Fig. 7. Comparison between SASW dispersion point sites and the filtered fundamental and first higher mode for the Saint Alban site.

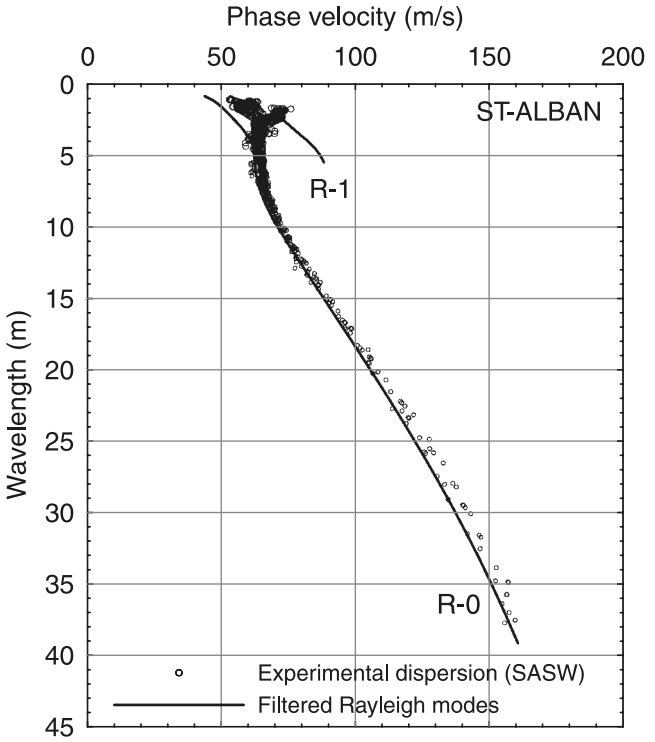

affects the shear-wave velocity profiles. To dissociate the effect of Poisson's ratio from the multi-mode problem, the V_s profile obtained by Lefebvre et al. (1994) is compared in Fig. 9 with the profiles obtained using the filtered dispersion curves with the proposed Poisson's ratios that with $\nu = 0.30$. The profile of Lefebvre et al. and that obtained in this study for the same Poisson's ratio ($\nu = 0.30$) show an important difference in the first 3 m of the deposit, and even at greater depth, due to the multi-mode problem only. The difference produced by the Poisson's ratio is not very important at depths of between 0 and 4 m because the dispersion curve does not vary significantly with variation of the Poisson's ratio at short wavelengths (Fig. 2). At depths greater than 4 m, however, the difference in shear-wave velocity produced by the Poisson's ratio becomes important and varies between 10% and 30%.

Bersimis-II site

SASW tests were performed in November 1991 on an embankment located at the Bersimis-II site on the north shore of the St. Lawrence River. The dyke was 15 m in height with a crest 5.5 m wide, slopes of 2H:1V, and a core of compacted clay. The SASW test was performed on the dyke crest with receiver spacings of 4, 8, 16, 32, and 64 m.

Reanalysis of the SASW records obtained at the Bersimis-II site using the filtering techniques described earlier in the text indicates an important participation of the higher Rayleigh modes (Fig. 10). The fundamental (R-0), first (R-1), and second (R-2) higher modes evaluated using the multiple filter and time-variable filter techniques are compared in Fig. 10 with the experimental points before filtration. At

Fig. 8. Comparison of the filtered dispersion curves of the fundamental and first higher Rayleigh modes with those evaluated theoretically for two sets of V_s and ν profiles.

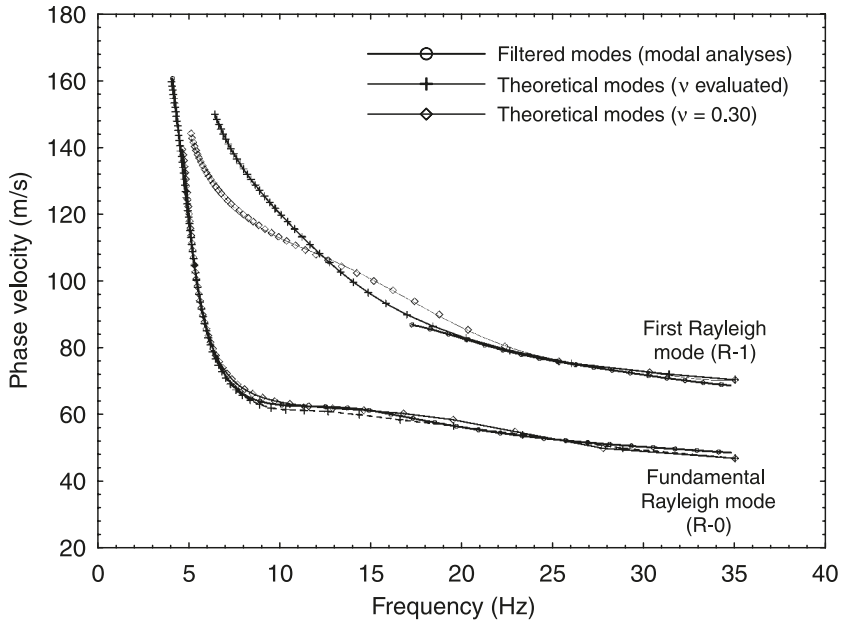

Fig. 9. Comparison between the Lefebvre et al. (1994) V_s profile and those obtained in this study using different Poisson's ratio profiles.

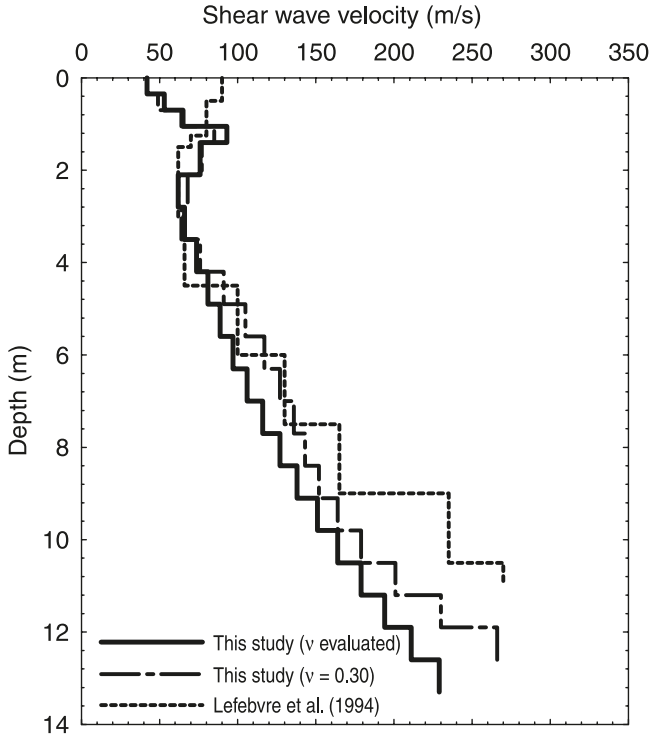

Fig. 10. Comparison between SASW dispersion point sites and the filtered fundamental and higher modes at the Bersimis-II site.

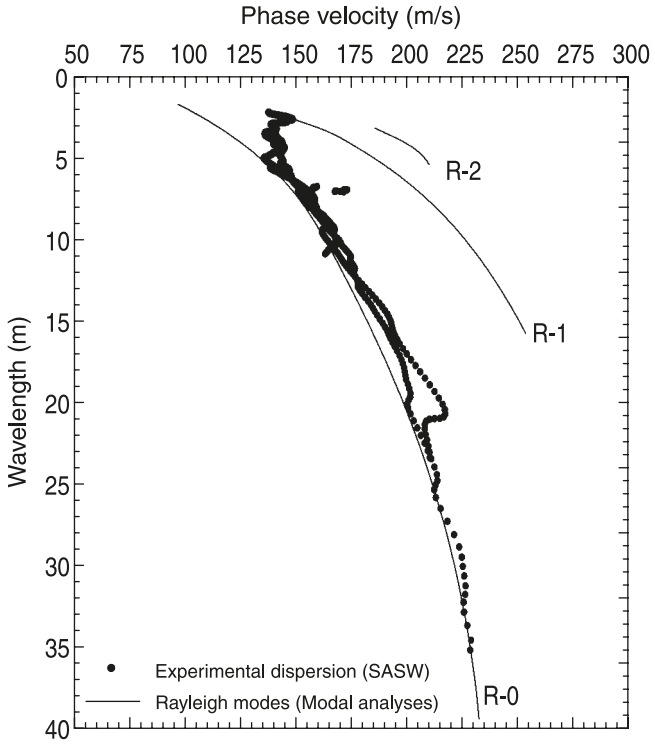

wavelengths greater than 6 m, the filtered R-0 dispersion curve coincides approximately with the average established by the experimental points before treatment, indicating a dominance of the fundamental mode. For wavelengths less than 6 m, the velocities of the fundamental mode are lower than the untreated values, indicating a significant participation of higher Rayleigh modes.

In this case, the determination of the fundamental Rayleigh mode and an important part of the first higher mode allows for good evaluation of the Poisson's ratio profile and a more accurate V_s profile. Figure 11*a* shows the V_s profiles evaluated for three different Poisson's ratio profiles presented in Fig. 11*b* using a trial-and-error process described

Fig. 11. V_s profiles obtained using different Poisson's ratio profiles at the Bersimis-II site.

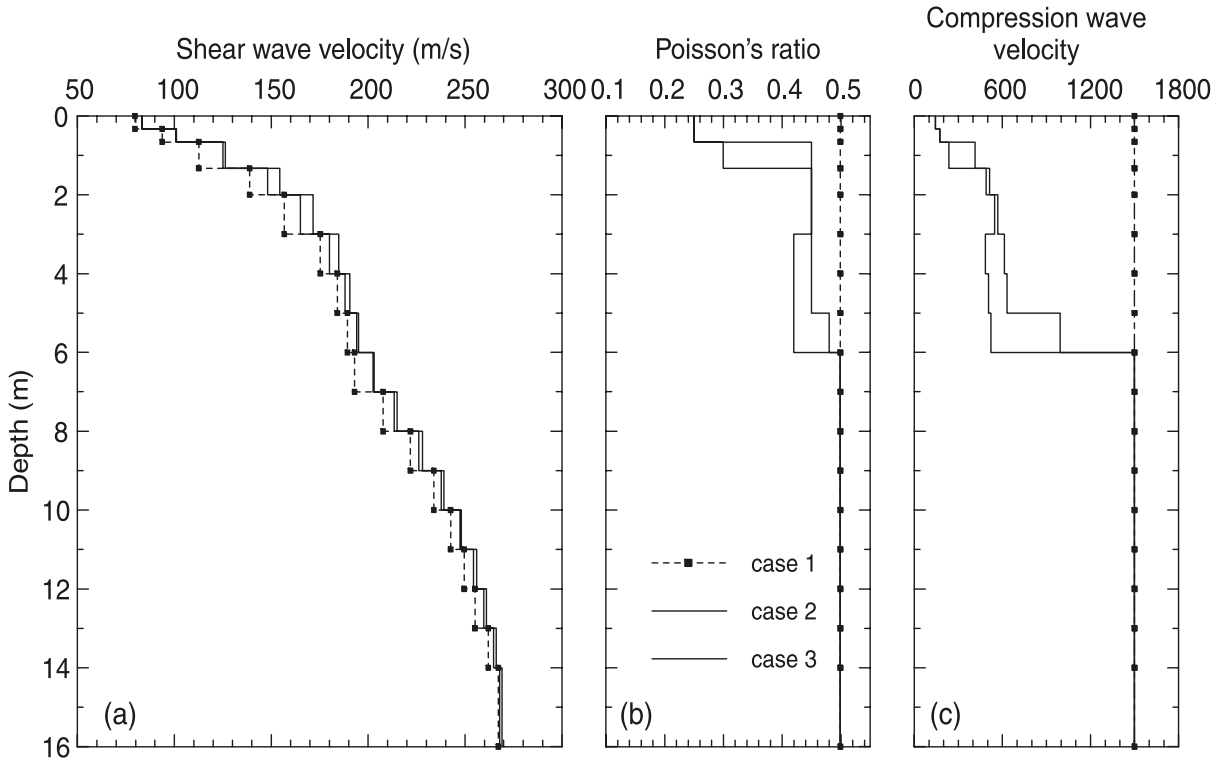

Fig. 12. Comparison of the filtered dispersion curves of the fundamental and first higher Rayleigh modes with those evaluated theoretically for three sets of V_s and ν profiles (Fig. 11).

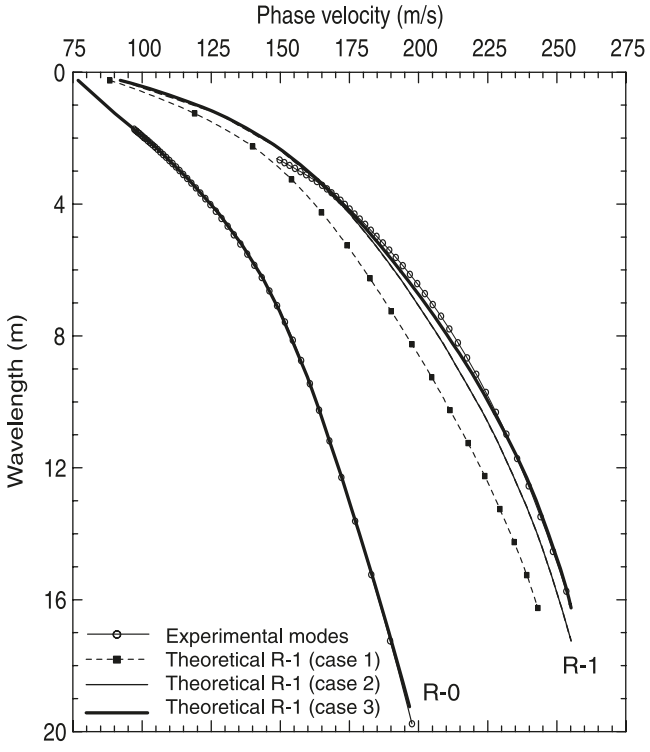

at the beginning of this paper. The V_p profiles are also presented in Fig. 11*c*.

The second and third Poisson's ratio profiles (cases 2 and 3 in Fig. 11) are relatively similar and involve a difference in shear-wave velocity varying between 1% and 5% (Fig. 11*a*). The difference between the first V_s profile, calculated for a constant compression wave velocity of 1500 m/s ($\nu \approx 0.5$), and the other cases is, however, more important and varies between 3% and 12%.

The theoretical Rayleigh modes evaluated from the corresponding pair of V_s and ν profiles are compared in Fig. 12 with the experimental filtered dispersion curves. The theoretical first higher mode of case 3 agrees closely with the filtered mode and differs by no more than 2 m/s (1%). This indicates that the shear-wave velocity profile of case 3 and the corresponding Poisson's ratio are an optimal solution of the filtered dispersion curves evaluated from the experimental records.

Conclusion

The effect of Poisson's ratio in construction of the theoretical dispersion curve has been examined using a number of ideas and experimental profiles. The determination of the higher Rayleigh modes from spectral analysis of surface waves (SASW) records obtained at two experimental sites has then been used to demonstrate the possibility of evaluating the Poisson's ratio profile and eventually determining a more accurate V_s profile when using a multi-mode inversion process.

The main conclusions from this study are summarized as follows:

(1) In the inversion process, the impact of Poisson's ratio in construction of the theoretical dispersion curves for conditions generally encountered in the field appears to be

significantly more important than that demonstrated for homogeneous conditions (Richart et al. 1970) or for a two-layer system (Nazarian 1984).

(2) The error in construction of theoretical dispersion curves and eventually in a V_s profile resulting from a Poisson's ratio inaccuracy, depends not only solely on the magnitude of the inaccuracy but also on the rate of V_s increase with an increase in depth and the pattern of V_s variation with depth, especially in the top layers.

(3) The inversion of a dispersion curve corresponding to the fundamental Rayleigh mode (R-0) leads to different V_s profiles depending on the Poisson's ratio assumption. However, these different V_s profiles correspond to different higher Rayleigh mode dispersion curves.

(4) Surface-wave testing would lead to a more accurate V_s profile if the techniques used to evaluate the fundamental Rayleigh mode dispersion curve do not eliminate the higher modes contribution, but instead isolate and determine the dispersion curves for the different Rayleigh modes contributing to the experimental records.

(5) A multi-mode inversion process using at least one higher mode in addition to the R-0 dispersion curve would help determine the Poisson's ratio profile, leading to a more accurate or optimal V_s profile.

(6) Multiple filters and time-variable filters are efficient techniques to isolate and extract the dispersion curves corresponding to the different Rayleigh modes contributing to the field records.

(7) At the very least, when a multi-mode inversion is not performed, the assumption of Poisson's ratio should be made with great care based on all available information. Even when a large portion of the soil profile is below the water table and saturated, the assumption of Poisson's ratio between ground surface and the water table may have an impact on the V_s profile.

Acknowledgments

The work presented in this paper was partly supported by the Natural Sciences and Engineering Research Council of Canada. Testing in the field was supported by Hydro-Québec.

References

Addo, K.O., and Robertson, P.K. 1994. Shear-wave velocity measurement of soils using Rayleigh waves. Canadian Geotechnical Journal, **29**: 558–568. doi:10.1139/t92-063.

Aki, K., and Richardson, P.G. 1980. Quantitative seismology: theory and methods. Freeman and Co., San Francisco, Calif.

Davidovici, V. 1985. Génie parasismique. École Nationale des Ponts et Chaussées, Paris. 1105 pp.

Dunkin, J.W. 1965. Computation of modal solutions in layered elastic media at high frequencies. Bulletin of the Seismological Society of America, **55**: 335–358.

Dziewonski, A.M., Bloch, S., and Landisman, M. 1969. A technique for the analysis of transient signals. Bulletin of the Seismological Society of America, **59**: 427–444.

Foti, S. 2000. Multistation methods for geotechnical characterization using surface waves. Dottoratody Ricercain Ingegneria Geotecnica, Universitàdegli Studidi Genova, Genova, Italy. 106 pp.

Ganji, V., Gucunski, N., and Nazarian, S. 1998. Automated inversion procedure for spectral analysis of surface waves. Journal of Geotechnical and Geoenvironmental Engineering, ASCE, **124**: 757–770. doi:10.1061/(ASCE)1090-0241(1998)124:8(757).

Gucunski, N., and Woods, R.D. 1992. Numerical simulation of the SASW test. Soil Dynamics and Earthquake Engineering, **11**: 213–227. doi:10.1016/0267-7261(92)90036-D.

Hardin, B.O., and Drnevich, V.P. 1972. Shear modulus and damping in soils: design equation and curves. Journal of the Soil Mechanics and Foundations Division, ASCE, **98**: 667–692.

Haskell, N.A. 1953. The dispersion of surface waves in multilayered media. Bulletin of the Seismological Society of America, **43**: 17–43.

Heisey, J.S. 1982. Determination of in-situ shear waves velocity from spectral-analysis-of-surface-waves, Ph.D. thesis, The University of Texas at Austin, Austin, Tex. 300 pp.

Jones, R. 1958. In-situ measurement of dynamic properties of soil by vibration methods. Géotechnique, **8**: 1–21.

Karray, M. 1999. Utilisation de l'analyse modale des ondes de Rayleigh comme outil d'investigation géotechnique in-situ. Thèse de doctorat en génie civil, Département de génie civil, Université de Sherbrooke, Sherbrooke, Que. 275 pp.

Kausel, E., and Roësset, J.M. 1981. Stiffness matrices for layered soils. Bulletin of the Seismological Society of America, **71**: 1743–1761.

Knopoff, L. 1964. A matrix method for elastic waves problems. Bulletin of the Seismological Society of America, **54**: 431–438.

La Rochelle, P., Trak, B., Tavenas, F., and Roy, M. 1974. Failure of a test embankment on a sensitive Champlain clay deposit. Canadian Geotechnical Journal, **11**: 142–164. doi:10.1139/t74-009.

Lefebvre, G., and Karray, M. 1998. New developments in in-situ characterization using Rayleigh waves. *In* Proceedings of the 51st Canadian Geotechnical Conference, Edmonton, Alta., 4–7 October 1998. Canadian Geotechnical Society, Alliston, Ont. Vol. 2, pp. 821–828.

Lefebvre, G., Leboeuf, D., Rahhal, M.E., Lacroix, A., Warde, J., and Stokoe, K.H., II. 1994. Laboratory and field determinations of small-strain shear modulus for a structured Champlain clay. Canadian Geotechnical Journal, **31**: 61–70. doi:10.1139/t94-007.

Nazarian, S. 1984. In-situ determination of elastic moduli of soil deposits and pavement systems by spectral-analysis-of-surface-waves method. Ph.D. Dissertations and thesis, The University of Texas at Austin, Austin, Tex. 452 pp.

Nazarian, S., and Stokoe, K.H. 1985. In-situ determination of elastic moduli of pavement systems by spectral-analysis-of-surface-waves methode (practical aspects). Research report 368-1F, Center for Transportation Research, The University of Texas at Austin, Austin, Tex. 161 pp.

Nelder, J.A., and Mead, R. 1964. A simplex method for function minimization. The Computer Journal, **7**: 308–313.

Park, C.B., Miller, R.D., and Xia, J. 1999. Multichannel analysis of surface waves. Geophysics, **64**: 800–808. doi:10.1190/1.1444590.

Richart, F.E., Jr., Hall, J.R., and Woods, R.D. 1970. Vibrations of soils and foundations. Prentice Hall Inc., Englewoods Cliffs, N.J. 414 pp.

Robertson, P.K., Sasitharan, S., Cunnig, J.C., and Sego, D.C. 1995. Shear-wave velocity to evaluate in-situ state of Ottawa sand. Journal of Geotechnical Engineering, ASCE, **121**: 262–273. doi:10.1061/(ASCE)0733-9410(1995)121:3(262).

Schwab, F. 1970. Surface-waves computation: Knopoff's method. Bulletin of the Seismological Society of America, **60**: 1491–1520.

Seed, H.B., and Idriss, I.M. 1970. Soil moduli and damping factors for dynamic reponse analysis. Research Report EERC 7010,

Earthquake Engineering Research Center, University of California, Berkeley, Calif.

Sharma, H.D., Dukes, M.T., and Olsen, D.M. 1990. Field measurements of dynamic moduli and Poisson's ratios of refuse and underlying soils at a landfill site. *In* Geotechnics of waste landfills — theory and practice. *Edited by* A. Landva and G.D. Knowles. American Society for Testing and Materials, Philadelphia, Penn., Special Technical Publication STP 1070. pp. 57–70.

Stokoe, K.H., Wright, S.G., Bay, J.A., and Roësset, J.M. 1994. Characterization of geotechnical sites by SASW method. *In* Proceedings of the 13th International Conference on Soil Mechanics and Foundation Engineering, New Delhi, 5–10 January 1994. A.A. Balkema, Rotterdam, the Netherlands. Vol. 1, pp. 15–25.

Tokimatsu, K., Tamura, S., and Kojima, H. 1992. Effects of multiple modes on Rayleigh wave dispersion characteristic. Journal of Geotechnical Engineering, ASCE, **118**: 1529–1543. doi:10.1061/(ASCE)0733-9410(1992)118:10(1529).

Vardoulakis, I., and Vrettos, C.H. 1988. Dispersion law of Rayleigh-type waves in a compressible Gibson half-space. International Journal for Numerical and Analytical Methods in Geomechanics, **12**: 639–655. doi:10.1002/nag.1610120606.

Youd, T.L., Idriss, I.M., Andrus, R.D., Arango, I., Castro, G., Christian, J.T., Dobry, R., Finn, W.D.L., Harder, L.F., Hynes, M.E., Ishihara, K., Koester, J.P., Liao, S.S.C., Marcuson, W.F., Martin, G.R., Mitchell, J.K., Moriwaki, Y., Power, M.S., Robertson, P.K., Seed, R.B., and Stokoe, K.H. 2001. Liquefaction resistance of soils: summary report from the 1996 NCEER and 1998 NCEER/NSF workshops on evaluation of liquefaction resistance of soils. Journal of Geotechnical and Geoenvironmental Engineering, ASCE, **127**: 297–313. doi:10.1061/(ASCE)1090-0241(2001)127:4(297).